DOI 10.5012/bkcs.2010.31.12.3852

Electrochemical Capacitance of Electrochemically Oxidized Ru Nanoparticles of Various Sizes on Platelet Carbon Nanofiber

Sechul Kim,[†] Byungjun Kim,[‡] Han-Gi Jeong,[‡] Choong Kyun Rhee,[†,§,*] and Tae-Hoon Lim[#]

[†]*Graduate School of Analytical Science and Technology, Chungnam National University, Daejeon 305-764, Korea*
[*]*E-mail: ckrhee@cnu.ac.kr*
[‡]*Department of Materials, Suntel, Cheongwon-Gun, Chungcheongbuk-Do 363-911, Korea*
[§]*Department of Chemistry, Chungnam National University, Daejeon 305-764, Korea*
[#]*Center for Fuel Cell Research, Korea Institute of Science and Technology, Seoul 136-791, Korea*
Received September 7, 2010, Accepted October 15, 2010

Key Words: Electrochemical capacitance, Ruthenium, Nanoparticle, Ruthenium oxide, Particle size

Hydrous ruthenium dioxide (RuO_2) has been highlighted as an electrode material of electrochemical capacitors. The capacitive charging process of hydrous RuO_2 consists of two routes: electrochemical double layer capacitance and pseudocapacitance. In particular, the pseudocapacitance has been emphasized due to a highly applicable capability ascribed to the following reversible redox reaction:[1]

$$RuO_2 + \delta H^+ + \delta e^- \leftrightarrow RuO_{2-\delta}(OH)_\delta, \text{ where } 0 \le \delta \le 2.$$

The performance of a hydrous RuO_2 capacitor has been proposed to be determined by the proton-electronic conduction of the material.[1-4] The hydrous regions of RuO_2 are responsible for proton conduction, while the crystalline forms determine electronic conduction between the particles. Because an annealing process to obtain a crystalline RuO_2 causes a loss of water, a simultaneous achievement of proton conduction and electronic conduction would be one of the key elements in its application to electrochemical capacitor electrodes. In an effort to obtain highly capacitive RuO_2, various attempts have been tried: adjustment of RuO_2 particle size,[5] optimization of RuO_2 layer thickness[6] and employment of conductive supports such as carbon materials.[5,7-11]

This work presents the variation of electrochemical capacitance of electrochemically oxidized RuO_2 as a function of particle size. Ru nanoparticles dispersed on platelet carbon nanofiber (PCNF), the size of which ranged from 5.9 to 1.6 nm, were electrochemically oxidized and evaluated as a capacitor. The main focus of this work is the utilization efficiency of Ru in pseudocapacitive charging process along with Ru nanoparticle size.

Figure 1 shows typical transmission electron micrographs of Ru nanoparticles dispersed on PCNF. The sizes and shapes of Ru nanoparticles depended clearly on the pH of ethylene glycol reducing medium. In the synthesis of Ru nanoparticles, ethylene glycol reduced the precursor Ru^{3+} ions to nanoparticles, and the glycolate (the product of the reduction reaction) determined the nanoparticle size as a stabilizer. Adjustment of the reducing medium pH determined the concentration of anionic glycolates, thus the Ru nanoparticle size. Figure 1(e) demonstrates a distribution of the Ru nanoparticle sizes prepared at pH 1.6,

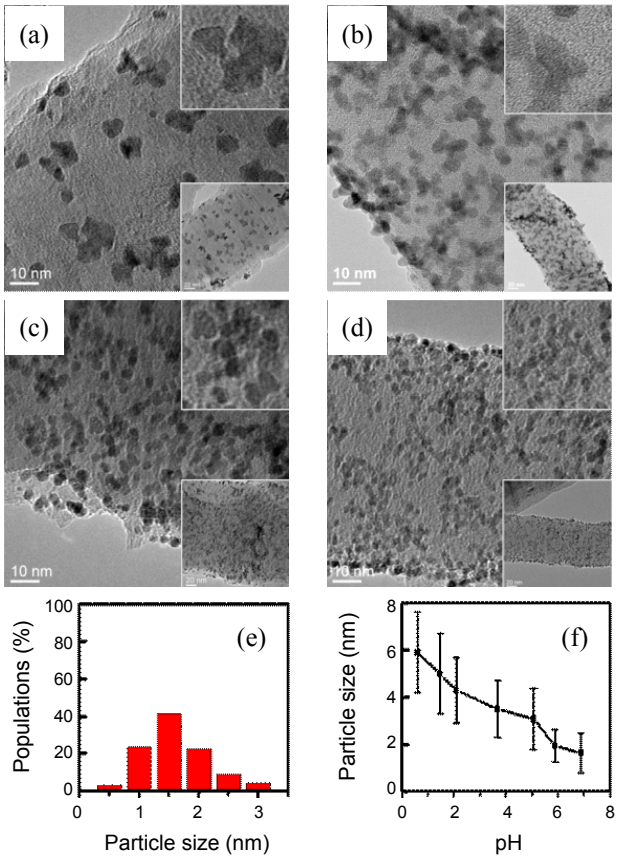

Figure 1. TEM micrographs of Ru nanoparticles synthesized in ethylene glycol reducing medium: (a) 5.9 nm, (b) 4.3 nm, (c) 3.5 nm, and (d) 1.9 nm. (e) Typical size distribution of Ru nanoparticles synthesized at pH 1.6. (f) The variation of Ru nanoparticle size as a function of reducing medium pH.

and Figure 1(f) displays the variation of Ru nanoparticle sizes as a function of reducing medium pH. As the pH increased from 0.6 to 6.9, the Ru nanoparticle size decreased from 5.9 to 1.6 nm. When the particle size was relatively large (pH < 2), on the other hand, the shapes of Ru nanoparticles were irregular as shown in Figure 1(a). In the pH range of 2 - 5, two or at most three nanoparticles aggregated (Figure 1(b)). When pH was

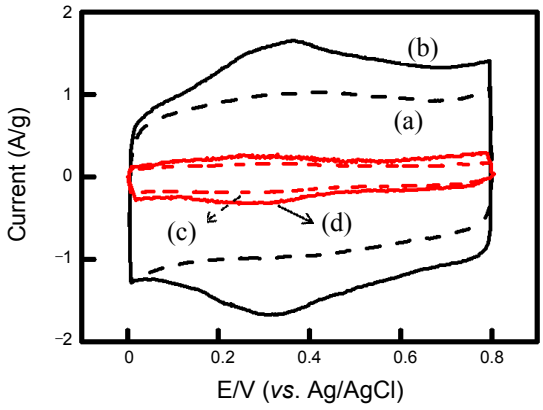

Figure 2. Cyclic voltammograms of Ru nanoparticles (1.6 nm) on PCNF electrochemically oxidized at 1.1 V for 30 min in 0.5 M H_2SO_4 solution: (a) before and (b) after the electrochemical oxidation. (c) and (d) are the cyclic voltammograms of PCNF before and after the electrochemical oxidation, respectively. Scan rate: 10 mV/s.

higher than 5, however, the Ru nanoparticles appear spherical and individual as demonstrated in Figure (c) and (d). In a reducing medium whose pH was higher than 7, the reduction of Ru precursor ions did not take place, so that Ru nanoparticles whose size was less than 1 nm was not available. The loaded amount of dispersed Ru nanoparticles on PCNF was 10 ± 0.5% of the total weight of the electrode material, regardless of size. The specific reason for the usage of PCNF simple in terms of structure is to avoid possible complicate problems associated with high surface area carbon materials such as Vulcan-72R.

Conversion of Ru nanoparticles to Ru oxide nanoparticles was performed by an electrochemical oxidation at 1.1 V for 30 min in 0.5 M H_2SO_4 solution. Figure 2(a) compares cyclic voltammograms of Ru nanoparticles (1.6 nm) and PCNF before and after the electrochemical oxidation. The cyclic voltammogram of Ru nanoparticles on PCNF before the electrochemical oxidation (Figure 2(a)) was rectangular, indicating that only an electrochemical double layer capacitive charging process, not a pseudocapacitive charging process, was operational. After the electrochemical oxidation, the voltammogram changed to the one (Figure 2(b)) with a broad redox couple at 0.32 V, denoting that a pseudocapacitive charging process took place. Furthermore, the electrochemical double layer charging process enhanced also as revealed by an increase in the current at 0.7 V by a factor of 1.3. Therefore, the electrochemical oxidation of Ru nanoparticles to oxidized nanoparticles increased the electrochemical capacitance obviously.

The contribution of PCNF to the total capacitance of Ru oxide on PCNF should be considered. Figure 2(c) and (d) compares the cyclic voltammograms of PCNF before and after the electrochemical oxidation: the contribution of the as-received PCNF to the total capacitance was roughly 20%. After the electrochemical oxidation, the modification of the PCNF support was not significant as shown in Figure 2(d), even though small pseudocapacitive peaks were apparent at 0.3 V. Thus, it is conclusive that the enhancement of the capacitance of the electrochemically oxidized Ru nanoparticles on PCNF came mainly from the conversion of metallic Ru nanoparticles to oxidized

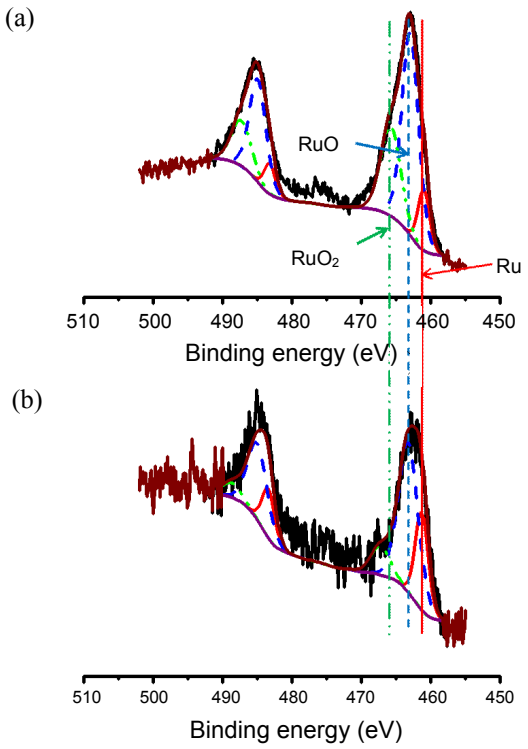

Figure 3. XPS spectra of Ru nanoparticles (2.9 nm) on PCNF electrochemically oxidized at 1.1 V for 30 min in 0.5 M H_2SO_4 solution: (a) before and (b) after the electrochemical oxidation.

nanoparticles. The capacitance values reported hereafter are the ones corrected by subtracting the contribution of PCNF from the observed capacitances.

Figure 3 shows the typical XPS spectra of Ru nanoparticles (2.9 nm) before and after the electrochemical oxidation. There were two Ru $3p_{3/2}$ and $3p_{1/2}$ peaks at 463 and 485 eV, respectively. In the peak of Ru $3p_{3/2}$, three components of Ru were identified to be metallic Ru at 461.9 eV, RuO at 463.6 eV, and RuO_2 at 465.9 eV. Before the electrochemical oxidation, the peak area ratio of Ru oxides to metallic Ru was 2.18 ± 0.07, indicating that most of Ru within the sampling depth of XPS (~1 nm) was Ru oxide species. After the electrochemical oxidation, the peak area ratio increased to 2.82 ± 0.06, regardless of Ru nanoparticle size, implying that the electrochemical oxidation to oxidized Ru nanoparticles was effective.

Figure 4(a) shows the variation in the capacitance of electrochemically oxidized Ru nanoparticles of various sizes on PCNF in 0.5 M H_2SO_4 solution as a function of voltammetric scan rate. The capacitance depended evidently on the particle size of oxidized Ru nanoparticles and scan rate. The variations in the capacitance values showed two distinctive features. When the sweep rate was higher than 50 mV/s, the observed capacitance remained fairly constant. In contrast, the scan rates lower than 50 mV/s resulted in a significant increase in capacitance. This particular behavior is due to the independence of electrochemical double layer charging on voltammetric scan rate and the slow kinetics of pseudocapacitive charging, i.e., irreversible faradaic reaction.[12] In the following discussion, the capacitance measured at 5 mV/s will be used. In any circumstances, as the

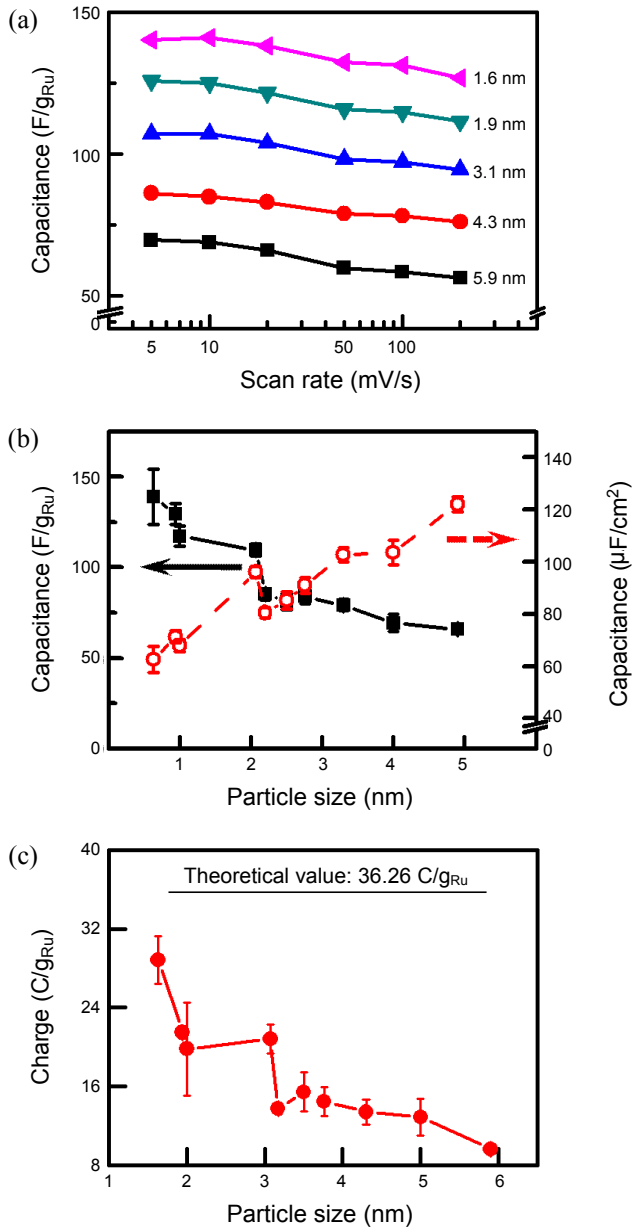

Figure 4. (a) The dependence of capacitance of electrochemically oxidized Ru nanoparticles on voltammetric scan rate. (b) The dependence of capacitance of electrochemically oxidized Ru nanoparticles on particle size. (c) The dependence of pseudocapacitive charge of electrochemically oxidized Ru nanoparticles on particle size. The theoretical pseudocapacitance is an estimated value assuming the pseudocapacitive process is $RuO_2 + 2H^+ + 2e \rightarrow Ru(OH)_2$.

particle size decreased, both capacitances of electrochemical double layer and pseudocapacitance certainly increased.

Figure 4(b) is a plot of particle size *versus* capacitance of electrochemically oxidized Ru nanoparticles. The mass specific capacitances (F/g$_{Ru}$) increased as the particle size decreased. Although the total capacitance of oxidized Ru nanoparticles in the range of 5.9 - 3.5 nm remained in the range of 70 - 80 F/g$_{Ru}$, the capacitance increased rapidly from ~100 F/g$_{Ru}$ (3 nm) to ~140 F/g$_{Ru}$ (1.6 nm). The ratio of electrochemical double layer capacitance to pseudocapacitance was always approximately 2, indicating that the contribution of pseudocapacitance to the total capacitance was about one-third. Although the surface area of the oxidized Ru nanoparticles increased by a factor of 14 as the size decreased from 5.9 to 1.6 nm, the capacitance increased by a factor of 2. This particular observation supports that the observed mass specific capacitance was not naively proportional to the surface area of the oxidized Ru nanoparticles, and denotes that only a simple geometrical factor did not operate in the two capacitive charging processes as a function of particle size. On the other hand, the surface area specific capacitances (μF/cm^2) decreased as the size decreased as shown in Figure 4(b). The surface areas of oxidized nanoparticles were calculated with the sizes measured using TEM. The value of the surface area specific capacitance diminished from 138 μF/cm^2 (5.9 nm) to 57 μF/cm^2 (1.6 nm) monotonically. To compare the results obtained in this work with a value of 12 nm Ru oxide nanoparticle (197 μF/cm^2) reported by Sugimoto,[13] an extrapolation to 12 nm was performed using the line of surface area specific capacitance *versus* particle size in Figure 4(b), and the extrapolated value was ~200 μF/cm^2, practically identical to the reported one.

Figure 4(c) shows the variation in pseudocapacitive charge as a function of particle size. When the particle size was smaller than 3 nm, the pseudocapacitive charge increased rapidly, indicating that more Ru was involved in the pseudocapacitive charging process. Assuming the pseudocapacitive process was $RuO_2 + 2H^+ + 2e \rightarrow Ru(OH)_2$, the fraction of Ru involved in the pseudocapacitive process was estimated. The fraction increased approximately from 0.3 to 0.8, when the particle size increased from 5.9 to 1.6 nm. Thus, as the particle size becomes smaller, more Ru clearly participates in the pseudocapacitive charging process.

In summary, the electrochemical oxidation of Ru nanoparticles increased the capacitance, in particular pseudocapacitance of Ru oxide species. As the particle size decreased from 5.9 nm to 1.6 nm, the capacitance increased by a factor of 2. Such an increase was due to the increase in the Ru fraction participating in pseudocapacitive charging process and electrochemical double layer capacitance related to surface area. In particular, when the Ru nanoparticle size was 1.6 nm, approximately 80% of Ru notably participated in pseudocapacitive charging process. Also, a simple geometrical surface area was not only a factor determining the capacitance of oxidized Ru nanoparticles.

Experimental Section

Preparation of Ru oxide nanoparticles on PCNF was carried out by the synthesis of Ru nanoparticles on the carbon support using polyol method,[14] followed by electrochemical oxidation of the metal nanoparticles. Details of the synthetic route are as follows: (1) 1.492 g of $RuCl_3 \cdot xH_2O$ (98.5%, Wako, Japan) was dissolved in 100 mL of ethylene glycol (99.5%, Wako, Japan) by heating, (2) after adding PCNF (supplied from Suntel, Korea)[15] into the Ru precursor solution, the pH of the reducing medium was adjusted to a proper pH (0.6 - 6.8) by adding 1 M NaOH ethylene glycol solution, (3) the mixture was refluxed at 200 °C for 3 hrs, and (4) the solid portion after reflux was filtered, washed with water until the pH of the washing water reached to 7, dried in a vacuum oven for 24 hrs, and grinded.

The Ru nanoparticles supported on PCNF were characterized

using a transmission electron microscope (TEM, JEM-2010F, JEOL) and a thermal gravimeter (TA instrument, SDT 2960 Simultaneous DTA-TGA). The diameters of Ru nanoparticles were measured from more than 300 nanoparticles in TEM images. The total gravimetric amounts of Ru nanoparticles were obtained by quantifying the residues (RuO_2) after burning off the carbon support.

In capacitance measurements, a conventional three electrode system was employed. Specifically, the working electrode was prepared by spreading a slurry of Ru nanoparticles on PCNF, 5% Nafion solution (Wako) and water on a Au disk electrode, followed by drying under an IR lamp.[14-15] The counter electrode was a Pt gauze and the reference electrode was a home-made Ag/AgCl electrode in 1.0 M NaCl. The potential reported in this work is against the reference electrode. The capacitance of the Ru nanoparticle was measured using cyclic voltammetry in 0.5 M H_2SO_4 solution (95 ~ 97%, Merck, Germany).

Acknowledgments. This work was financially supported by Korean Institute of Science and Technology (contract number: 2E20670-08-081). The authors appreciate the permission of Center for Research Facilities, Chungnam National University, to the instrument of X-ray photoelectron spectroscopy used in this work.

References

1. Barbieri, O.; Hahn, M.; Foelske, A.; Kotz, R. *J. Electrochem. Soc.* **2006**, *153*, A2049.
2. Zheng, J. P.; Xin, Y. *J. Power Sources* **2002**, *110*, 86.
3. Sugimoto, W.; Iwata, H.; Yokoshima, K.; Murakami, Y.; Takasu, Y. *J. Phys. Chem. B* **2005**, *109*, 7330.
4. Zheng, J. P.; Cygan, P. J.; Jow, T. R. *J. Electrochem. Soc.* **1995**, *142*, 2699.
5. Chang, K.-H.; Hu, C.-C. *Electrochem. Solid-State Lett.* **2004**, *7*, A466.
6. Jang, J. H.; Kato, A.; Machida, K.; Naoi, K. *J. Electrochem. Soc.* **2006**, *153*, A321.
7. Kim, H.; Popov, B. N. *J. Electrochem. Soc.* **2003**, *150*, A1153.
8. Min, M.; Machida, K.; Jang, J. H.; Naoi, K. *J. Electrochem. Soc.* **2006**, *153*, A334.
9. Kim, I.-H.; Kim, J.-H.; Lee, Y.-H.; Kim, K.-B. *J. Electrochem. Soc.* **2005**, *152*, A2170.
10. Kim, Y.-T.; Tadai, K.; Mitani, T. *J. Mater. Chem.* **2005**, *15*, 4914.
11. Miller, J. M.; Dunn, B. *Langmuir* **1999**, *15*, 799.
12. Sugimoto, W.; Iwata, H.; Murakami, Y.; Takasu, Y. *J. Electrochem. Soc.* **2004**, *151*, A1181.
13. Sugimoto, W.; Kizaki, T.; Yokoshima, K.; Murakami, Y.; Takasu, Y. *Electrochim. Acta* **2004**, *49*, 313.
14. Kim, B.-J.; Kwon, K.; Rhee, C. K.; Han, J.; Lim, T.-H. *Electrochim. Acta* **2008**, *53*, 7744.
15. Kim, T.; Lim, S.; Kwon, K.; Hong, S.-H.; Qiao, W.; Rhee, C. K.; Yoon, S.-H.; Mochida, I. *Langmuir* **2006**, *22*, 9086.